Three-Port Lorentz Resonance Based Permittivity Sensor and Microwave Comparator

Abdul Jabbar[1], Rashad Ramzan[2], Omar Siddiqui[3], Muhammad Amin[3], Muhammad Ali Imran[1], Qammer H. Abbasi[1] and Masood Ur Rehman[1]

James Watt School of Engineering, University of Glasgow, UK[1]
National University of Computer and Emerging Sciences, Islamabad, Pakistan[2]
College of Engineering, Taibah University Medina, Saudi Arabia[3]

***Abstract*—This paper presents for the first time a compact three-port Lorentz resonance-based microstrip sensor for permittivity and moisture sensing, as well as refractive index comparison. The proposed sensor is verified by simulations and experiments. The resonant frequency of the designed sensor is 2.24 GHz. The proposed sensor has a quality factor of 102, sensitivity of 45.4 mm/refractive index unit, and figure-of-merit of 34.6. The sensitivity of the proposed sensor is quite superior to other resonance based sensors and a fair comparison is presented in this work. The proposed sensor can be used to find the permittivity of dielectric materials, the moisture content of plants, as well as can be used as a refractive index comparator.**

Keywords—Lorentz resonance, microstrip sensor, permittivity

I. INTRODUCTION

Sensor designing has always been of great interest for researchers since it is always crucial to detect real-time environmental phenomena [1]. Some of the prime features to be considered in a sensor design include high sensitivity, compact size, comfortability, and robustness in a harsh environment. There are several types of sensors which have their own importance in different application scenarios such as measurements of liquid solutions [2], [3], detection of volatile organic compounds [4], [5], gas sensing [6], material characterization, biology and nanotechnology [7], thickness and permittivity detection [8]-[12], temperature and strain sensing [13]-[15], as well as glucose and moisture sensing [16]-[21], to name but a few. Primarily, the perturbations in the nearby environment of a sensor impart an effect on the amplitude, phase and frequency response of the designed sensor, through which the material characterization can be done effectively.

In the area of microwave sensing, material characterization techniques can be divided into two main categories, i.e., resonant and non-resonant. The resonant methods are inherently narrowband and the material characterization can be carried out through the amplitude spectrum by analyzing the resonant frequency and quality factor of the sensor when loaded with the sample under test (SUT). These resonant methods are usually quite accurate and computationally less exhaustive [22]-[24]. On the other hand, non-resonant methods provide a general view of the material properties over a broad spectrum and require accurate calibration of the measurement setup over a wide spectrum [25]-[27].

The planar microwave sensors usually rely on resonance sensing, amongst which Lorentz resonance [28]-[33] is quite famous. In these sensors, a two-port or a single port microstrip structure is usually used with an open circuit stub or a wide patch that resonates at a particular frequency. The stub or patch is used to locate the SUT through which the reflection or transmittance resonance response of the sensor is changed, and sensing is performed.

This work is inspired by some recently reported works which employed Lorentz resonance to detect and characterize dielectric materials [28]-[33]. However, none of those designs provides the notion of constant reference keeping. Moreover, only one dielectric sample can be detected and characterized by those designs. However, in this paper, a compact three-port Lorentz resonance-based microstrip sensor is designed for the first time for permittivity detection and characterization. The high sensitivity and figure of merit (FOM) of the proposed sensor verify its utility for permittivity and moisture sensing. As the sensor consists of three ports, thus it has two inherent benefits. One is that the reference frequency is constantly maintained if one of the two output ports is unloaded. While the second benefit lies in the fact that two different dielectric samples can be characterized simultaneously if both output ports are loaded with different samples. Thus, in addition to permittivity detection, the proposed sensor design can be used as a microwave comparator (or refractive index comparator). For the sake of proof of concept, here only one of the two output ports is used to measure the SUT, while the other port is kept unloaded to maintain the reference value. A prototype is also developed and tested to verify the practicality of the proposed sensor.

II. DESIGN OF THE PROPOSED SENSOR

The prototype of the proposed sensor is shown in Fig. 1. It consists of three ports which are matched to 50 Ω. Port-1 is considered as the input port, while port-2 and port-3 are supposed to be the output ports. The design is symmetric and consists of an open circuit stub between the input port (port-1) and each output port (port-2 and 3).

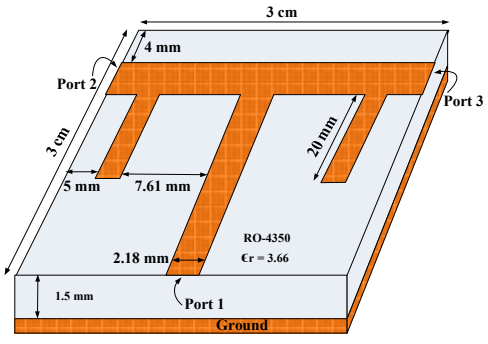

Fig.1. The design and prototype of the proposed three-port sensor.

The prototype has been designed on Rogers 4350B substrate with a dielectric constant of 3.66, thickness of 1.524 mm, and a dissipation factor of 0.0031. The optimized dimensions of the design are provided in Fig. 1, and the overall size of the sensor is chosen to be 3 cm × 3cm so that it is easily capable to accommodate solid dielectric samples on it. However, the design is easily scalable to a wide range of frequencies.

Each open circuit stub towards the output port is responsible for resonance as its electrical length becomes equal to quarter-wavelength. Both stubs are kept equal in length, thus the transmittance parameters (S21 and S31) overlap at the same resonance frequency (when the sensor is unloaded). The inherent resonance frequency of the proposed design is set at 2.24 GHz, and depends on the length of open stubs as well as the effective permittivity of the microstrip line given by (1):

$$f_r = \frac{c}{4L\sqrt{\varepsilon_e}} \quad (1)$$

where f_r is the resonance frequency, L is the length of open circuit stub and ε_e is the effective permittivity of the microstrip line.

III. SIMULATION RESULTS AND DISCUSSION

The proposed sensor was simulated in loaded (with SUT) and unloaded (without SUT) conditions. Since the design consists of three ports, thus two transmittance responses are available, i,e., S21 and S31. The sensor possesses two signatures for sensing and detection, one is the amplitude response, while the other is phase response. The amplitude and phase responses of the unloaded sensor are shown in Fig. 2a and b. However, in this work, only amplitude-based sensing is elucidated.

The amplitude response of a Lorentz resonator contains a distinctive feature i.e., the resonance dip (Fig. 2a) from which the spectral information and thus the material properties can be extracted. At 2.24 GHz, both open circuit stubs having equal length of 20 mm become quarter-wavelength long and resonate. Since an open circuit stub behaves as a short circuit with the least impedance at resonance, thus all the incoming energy from port-1 resonates in the stubs instead of moving towards the output ports. Consequently, a transmission null is obtained in the amplitude response at the resonance frequency. The resonance phenomenon is also depicted in the form of field distribution in Fig. 3, which further explicates that at the resonance frequency of 2.24 GHz, the stubs are in excited state.

In order to detect the permittivity or moisture content of a dielectric SUT, the stub towards port-3 is used for sample placement. If a dielectric sample is placed on the open stub, it perturbs the nearby fields of the loaded stub, thereby increasing the effective dielectric constant experienced by the open-stub, resulting in the redshift of the resonance profile. To preserve the reference value, the stub towards port-2 is left unloaded. This is because the resonance response of S21 and S31 is independent of each other, and the unloaded resonance (say S21) will not change its reference value even when the other pair is loaded (say S31). When an SUT is put on the stub towards port-3, the resonance curve (S31) experiences a redshift from the reference position and can easily be sensed.

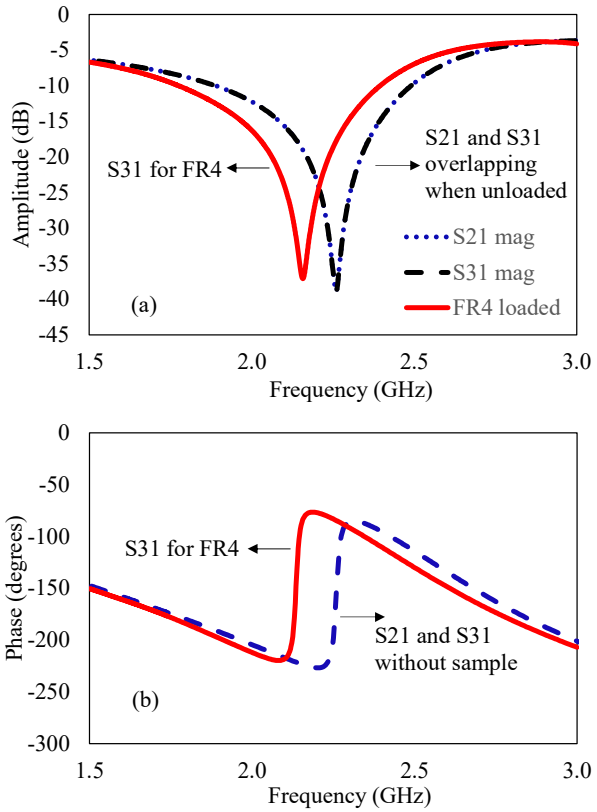

Fig. 2. The response of three port Lorentz sensor. (a) amplitude response showing transmission null for S21 and S31 at 2.24 GHz, and redshift for FR4 sample. (b) anomalous phase response with and without SUT.

In this work, the stub towards port-3 was loaded with a sample of FR4 with relative permittivity of 4.34 and thickness of 1.5 mm (while the stub towards port-2 was left unloaded to maintain the reference level). The resonance frequency of S21 (reference frequency 2.24 GHz) was unchanged, while the transmission dip of S31 moved to a lower frequency of 2.13 GHz as shown in Fig. 2a. This redshift of 110 MHz for FR4 sample is due to the increase in the effective permittivity of the loaded stub. The quality factor of the proposed sensor is 102. The sensitivity (m) of the sensor when loaded with FR4 was found to be 45.4 mm/RIU (Refractive Index Unit) using (2), which is much higher than many of the previously reported sensors as shown in Table I.

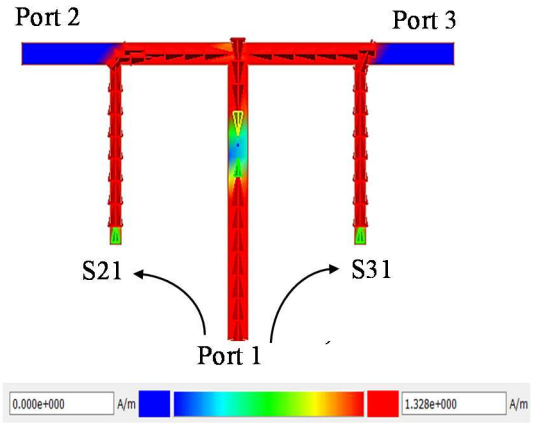

Fig. 3. The distribution of magnetic field strength shows that maximum energy flows through the open circuit stubs at the resonance frequency of 2.24 GHz.

TABLE I. Performance comparison of the proposed sensor with other related works.

Ref.	Sensitivity (mm/RIU)	FOM	Resonant frequency (GHz)
[9]	14.20	6.17	3.6
[10]	13.71	59.60	5.23
[11]	10.3	34.33	9.99
[12]	9.47	13.5	9.10
This work	**45.4**	**34.6**	**2.24**

$$m = \frac{\lambda_1 - \lambda_2}{n_2 - n_1} \tag{2}$$

Here n_1 and n_2 are the refractive indices corresponding to the relative permittivities of unloaded and loaded sensors respectively ($n = \sqrt{\varepsilon_r \mu_r}$, and $\mu_r = 1$). λ_1 is the wavelength corresponding to the resonance frequency of the unloaded sensor, while λ_2 corresponds to that of the loaded sensor. The FOM of the proposed sensor is 34.6 and is found using the relation $FOM = \frac{m\,(^{mm}/_{RIU})}{FWHM}$, where $FWHM$ is full width at half maximum of the amplitude response (S31). The sensitivity (m) is the linear slope of the resonance wavelength shift over the refractive index variation, whereas FOM takes further consideration of the resonant lineshape. The performance of the proposed sensor is quite good which is compared with some of the previously reported microstrip based sensors and is shown in Table I.

IV. FABRICATION AND MEASUREMENTS

The proposed sensor was fabricated on Rogers 4350B substrate as shown in Fig. 4 inset. The transmission characteristics were measured using a handheld Rohde & Schwarz ZVH8 vector network analyzer (VNA) having only real-time data analyzing capability. Since this VNA has no data saving feature, thus the measured response of the sensor was captured in the form of a real-time image and shown in Fig. 4. First, the sensor was measured unloaded and S31 was found to be at the resonance frequency of 2.28 GHz, while port-2 was terminated with 50 Ω load. A similar measurement was performed for S21 while keeping port-3 terminated. Both S21 and S31 were overlapping due to the equal length of stubs. After that, a small sample of FR4 (relative permittivity of 4.34) was cut with dimensions of 18 mm × 2 mm and thickness of 1.5 mm, was placed on the stub, and S31 was measured. The S31 response was shifted to a new resonance frequency of 2.055 GHz, showing a redshift of 255 MHz. The simulated and measured results show a relative difference within 3% and are in good agreement. The small deviation of the measured results is possibly due to fabrication imperfections and permittivity tolerances. From the shifted resonance frequency, the effective permittivity ε_e and subsequently, the real part of relative permittivity of the SUT can be found analytically using well-known relations (3) and (4) [34]:

$$\varepsilon_e = \frac{c^2}{16 L^2 f_r^2} \tag{3}$$

$$\varepsilon_r = \frac{2\varepsilon_e \sqrt{1+12\frac{H}{W}} - \sqrt{1+12\frac{H}{W}} + 1}{1+\sqrt{1+12\frac{H}{W}}} \tag{4}$$

Here H is the thickness of the substrate and W is the width of microstrip line. According to (3), the effective relative permittivity has a strong relationship with resonant frequency. As the frequency undergoes redshift in the presence of SUT, the effective permittivity increases and vice versa.

The measured values of relative permittivity for Rogers 4350 (unloaded) and loaded FR4 sample are found within 4% of their known values and are shown in Table II. For the sake of simplicity and concision, only FR4 sample was measured in this work with only one stub loaded with SUT, while keeping the other stub unloaded. In future work, more samples could be tested to generate multiple frequency shifts and a sensitivity curve.

Another striking utility of the same three-port sensor design is as a refractive index comparator, where both stubs can be loaded with different dielectric samples simultaneously. In that case, a three-port VNA is a preferred choice for measurements. The shift in the resonance frequency of S21 and S31 responses can then be used to estimate the corresponding relative permittivity analytically using (3) and (4). In this way, any two dielectric materials can be characterized and compared at the same time. Besides, for loss tangent characterization, the information about the slope of the phase response can be used. However, due to concision, it is not included in this work. Real-time refractive index comparison is anticipated to be performed as the extension of this work in more detail in near future, which will create insight for multiple dielectric sensing simultaneously with a single sensor design. Moreover, the proposed sensor design can also be extended to applications to detect changes in more materials properties such as loss and thickness.

TABLE II. Comparison of the nominal (known) and measured values of relative permittivities.

Material	f_r measured S31 (GHz)	ε_r (nominal)	ε_r (measured)	Relative difference (%)
Rogers 4350B	2.28	3.66	3.59	1.91
FR4	2.05	4.34	4.5	3.55

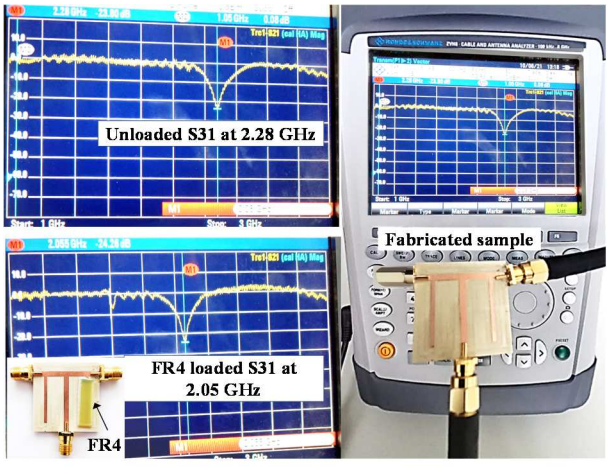

Fig. 4. Measurement setup along with the fabricated sample of the sensor. The unloaded sensor shows S31 dip at 2.28 GHz. While loading with FR4 sample, the resonance frequency dip shifts to 2.05 GHz.

V. CONCLUSION

In this paper, a compact three-port Lorentz resonance-based microstrip sensor is designed, fabricated, and tested. The high sensitivity and FOM of the proposed sensor verify its utility for detecting the permittivity of dielectric materials The sensing characteristics are analyzed in detail in this paper. The difference between extracted and the nominal values of dielectric constants lie within 4%. The extraction error mainly arises due to approximations in microstrip analytical formulas, fabrication imperfections, radiation in the open stub and permittivity tolerances. Moreover, since the proposed sensor involves three ports, thus it is innately a suitable candidate to be used as a refractive index comparator.

REFERENCES

[1] A. J. Baeumner, H. Cui, G. Gauglitz, M. C. Moreno-Bondi, S. Szunerits, and A. T. Woolley, "Advancements in sensor technology with innovative and significant research publications: how to write that perfect paper?" Springer, 2021.

[2] G. Gennarelli, S. Romeo, M. R. Scarfi, and F. Soldovieri, "A microwave resonant sensor for concentration measurements of liquid solutions," IEEE Sens. J., vol. 13, no. 5, pp. 1857–1864, 2013.

[3] Abdulkarim, Yadgar I., Lianwen Deng, Muharrem Karaaslan, Olcay Altıntaş, Halgurd N. Awl, Fahmi F. Muhammadsharif, Congwei Liao, Emin Unal, and Heng Luo. "Novel metamaterials-based hypersensitized liquid sensor integrating omega-shaped resonator with microstrip transmission line." Sensors 20, no. 3, 943, 2020.

[4] M. H. Zarifi, A. Sohrabi, P. M. Shaibani, M. Daneshmand, and T. Thundat, "Detection of volatile organic compounds using microwave sensors," IEEE Sens. J., vol. 15, no. 1, pp. 248–254, 2014.

[5] Slobodian, Petr, Pavel Riha, Robert Olejnik, Jiri Matyas, and Rostislav Slobodian. "Microstrip Resonant Sensor for Differentiation of Components in Vapor Mixtures." Sensors 21, no. 1, 298, 2021.

[6] X. Liu, S. Cheng, H. Liu, S. Hu, D. Zhang, and H. Ning, "A survey on gas sensing technology," Sensors, vol. 12, no. 7, pp. 9635–9665, 2012.

[7] R. Joffe, E. O. Kamenetskii, and R. Shavit, "Novel microwave near-field sensors for material characterization, biology, and nanotechnology," J. Appl. Phys., vol. 113, no. 6, p. 63912, 2013.

[8] C.-S. Lee and C.-L. Yang, "Thickness and permittivity measurement in multi-layered dielectric structures using complementary split-ring resonators," IEEE Sens. J., vol. 14, no. 3, pp. 695–700, 2013.

[9] L. Zhu, J. H. Fu, F. Y. Meng, X. M. Ding, L. Dong, and Q. Wu, "Detuned magnetic dipoles induced transparency in microstrip line for sensing," IEEE Trans. Magn., vol. 50, no. 1, pp. 1–4, 2013.

[10] X. Q. Lin, Z. Chen, J. W. Yu, P. Q. Liu, P. F. Li, and Z. D. Chen, "An EIT-based compact microwave sensor with double sensing functions," IEEE Sens. J., vol. 16, no. 2, pp. 293–298, 2015.

[11] R. Li, X. Kong, S. Liu, Z. Liu, and Y. Li, "Planar metamaterial analogue of electromagnetically induced transparency for a miniature refractive index sensor," Phys. Lett. A, vol. 383, no. 32, p. 125947, 2019.

[12] L. Zhu, L. Dong, F. Meng, J. Fu, and Q. Wu, "Influence of symmetry breaking in a planar metamaterial on transparency effect and sensing application," Appl. Opt., vol. 51, no. 32, pp. 7794–7799, 2012.

[13] Lu, Yang, Chams Baker, Liang Chen, and Xiaoyi Bao. "Group-delay-based temperature sensing in linearly-chirped fiber Bragg gratings using a Kerr phase-interrogator." Journal of Lightwave Technology 33, no. 2, 381-385, 2015.

[14] Ossa-Molina, Oscar, J. Duque-Giraldo, and Erick Reyes-Vera. "Strain sensor based on rectangular microstrip antenna: numerical methodologies and experimental validation." IEEE Sensors Journal, 2021.

[15] Nikbakhtnasrabadi, Fatemeh, Hatem El Matbouly, Markellos Ntagios, and Ravinder Dahiya. "Textile-Based Stretchable Microstrip Antenna with Intrinsic Strain Sensing." ACS Applied Electronic Materials 3, no. 5 (2021): 2233-2246.

[16] Yee, See Khee, Soon Chong Johnson Lim, Pih Shyan Pong, and Samsul Haimi Dahlan. "Microstrip defected ground structure for determination of blood glucose concentration." Progress In Electromagnetics Research C 99, 35-48, 2020.

[17] Mohammadi, P., A. Mohammadia, S. Demir, and A. Kara. "Compact Size, and Highly Sensitive, Microwave Sensor for Non-Invasive Measurement of Blood Glucose Level." IEEE Sensors Journal, 2021.

[18] Jain, Sweety. "Early Detection of Salt and Sugar by Microstrip Moisture Sensor Based on Direct Transmission Method." Wireless Personal Communications, 1-9, 2021.

[19] N. Y. Kim, R. Dhakal, K. K. Adhikari, E. S. Kim, and C. Wang, "A reusable robust radio frequency biosensor using microwave resonator by integrated passive device technology for quantitative detection of glucose level," Biosens. Bioelectron., vol. 67, pp. 687–693, 2015.

[20] Sharafadinzadeh, Niloofar, Mohammad Abdolrazzaghi, and Mojgan Daneshmand. "Highly sensitive microwave split ring resonator sensor using gap extension for glucose sensing." In 2017 IEEE MTT-S International Microwave Workshop Series on Advanced Materials and Processes for RF and THz Applications (IMWS-AMP), pp. 1-3. IEEE, 2017.

[21] A. Cataldo, G. Monti, E. De Benedetto, G. Cannazza, and L. Tarricone, "A non-invasive resonance-based method for moisture content evaluation through microstrip antennas," IEEE Trans. Instrum. Meas., vol. 58, no. 5, pp. 1420–1426, 2009.

[22] R. Ramzan, O. Siddiqui, A. Nauroze, and O. Ramahi, "A microstrip probe based on electromagnetic energy tunneling for extremely small and arbitrarily shaped dielectric samples," IEEE Antennas Wirel. Propag. Lett., vol. 14, pp. 1554–1556, 2015.

[23] H. Yoshikawa and A. Nakayama, "Measurements of complex permittivity at millimeter-wave frequencies with an end-loaded cavity resonator," IEEE Trans. Microw. Theory Tech., vol. 56, no. 8, pp. 2001–2007, 2008.

[24] K. Buell and K. Sarabandi, "A method for characterizing complex permittivity and permeability of meta-materials," in IEEE Antennas and Propagation Society International Symposium, vol. 2, pp. 408–411, 2002.

[25] L. Yousefi, H. Attia, and O. M. Ramahi, "Broadband experimental characterization of artificial magnetic materials based on a microstrip line method," Prog. Electromagn. Res., vol. 90, pp. 1–13, 2009.

[26] P. Queffelec, P. Gelin, J. Gieraltowski, and J. Loaec, "A microstrip device for the broad band simultaneous measurement of complex permeability and permittivity," IEEE Trans. Magn., vol. 30, no. 2, pp. 224–231, 1994.

[27] W. Barry, "A broad-band, automated, stripline technique for the simultaneous measurement of complex permittivity and permeability," IEEE Trans. Microw. Theory Tech., vol. 34, no. 1, pp. 80–84, 1986.

[28] O. Siddiqui, "Metal Detector Based on Lorentz Dispersion," IEEE Sens. J., vol. 21, no. 3, pp. 3784–3790, 2020.

[29] A. Jabbar, M. Omar, R. Ramzan, and O. F. Siddiqui, "Internet of Trees (IoTr): A Low-Cost Single Stub Lorentz Resonator For Plant Moisture Sensing," in 2021 International Bhurban Conference on Applied Sciences and Technologies (IBCAST), pp. 979–982, 2021.

[30] O. F. Siddiqui, R. Ramzan, M. Amin, M. Omar, and N. Bastaki, "Lorentz reflect-phase detector for moisture and dielectric sensing," IEEE Sens. J., vol. 18, no. 22, pp. 9236–9242, 2018.

[31] R. Ramzan, O. F. Siddiqui, M. W. Arshad, and O. M. Ramahi, "A complex permittivity extraction method based on anomalous dispersion," IEEE Trans. Microw. Theory Tech., vol. 64, no. 11, pp. 3787–3796, 2016.

[32] R. Ramzan, O. Siddiqui, M. Amin, N.Bastaki, "Plant Water Sensor." Patent No: 10605746; Granted 31 March, 2020, US Patent Office.

[33] O. Siddiqui, R. Ramzan, M. Amin, and O. M. Ramahi, "A non-invasive phase sensor for permittivity and moisture estimation based on anomalous dispersion," Sci. Rep., vol. 6, p. 28626, 2016.

[34] D. M. Pozar, Microwave engineering. John wiley & sons, 2011.